

Inertial effects of self-propelled particles: from active Brownian to active Langevin motion

Hartmut Löwen¹

Institut für Theoretische Physik II: Weiche Materie, Heinrich-Heine-Universität Düsseldorf, D-40225 Düsseldorf, Germany

(Dated: 31 October 2019)

Active particles which are self-propelled by converting energy into mechanical motion represent an expanding research realm in physics and chemistry. For micron-sized particles moving in a liquid (“microswimmers”), most of the basic features have been described by using the model of overdamped active Brownian motion. However, for macroscopic particles or microparticles moving in a gas, inertial effects become relevant such that the dynamics is underdamped. Therefore, recently, active particles with inertia have been described by extending the active Brownian motion model to active Langevin dynamics which include inertia. In this perspective article recent developments of active particles with inertia (“microflyers”) are summarized both for single particle properties and for collective effects of many particles. There include: inertial delay effects between particle velocity and self-propulsion direction, tuning of the long-time self-diffusion by the moment of inertia, effects of fictitious forces in non-inertial frames, and the influence of inertia on motility-induced phase separation. Possible future developments and perspectives are also proposed and discussed.

Invited **perspective article** for *The Journal of Chemical Physics*.

I. INTRODUCTION

The dynamics of self-propelled particles which are perpetually moving by converting energy (“fuel”) into mechanical motion represent a nonequilibrium phenomenon. Research in the last decades was not only driven by the broad range of applications (such as precision surgery, drug delivery and cargo transport on the micron-scale) but also from a more fundamental level in terms of identifying basic relevant models to describe the particle trajectories under nonequilibrium conditions. One of the first standard models in this respect is the Vicsek model of swarming proposed in 1995 by Vicsek and coworkers¹ which is by now a cornerstone in describing collective active matter systems. With the upsurge of synthetic colloidal Janus-like particles which create their own gradient in which they are moving, artificial microswimmers were considered as model systems for active matter. These micron-sized particles typically self-propel in a liquid at very low Reynolds number. Therefore the dynamics of these colloidal particles in a solvent is overdamped and one of the most popular descriptions is obtained by *active Brownian motion*^{2–4} combining solvent kicks described as Gaussian white noise and overdamped motion together with an effective self-propulsion force representing the particle self-propulsion. The active Brownian particle model has been tested against experimental data of self-propelled colloids^{2,5,6} and has been used also to describe and predict collective phenomena for colloids and bacteria⁷.

More recently, there have been developments to consider larger self-propelled particles or motion in low-density environment (gas instead of liquid). Then the motion is not any longer at low Reynolds number. In-

stead inertial effects are getting relevant in the dynamics and need to be included in the modelling. These inertia-dominated particles are “microflyers” rather than “microswimmers” since their dynamics is underdamped and rather corresponds to flying than swimming. Still the motion is affected by fluctuating random kicks of the surrounding medium. Correspondingly one can coin their dynamics as *active Langevin motion* rather than “active Brownian motion”. However, it is remarked here that sometimes in the literature^{8,9} the term “active Brownian motion” is used in a more general sense including also underdamped Langevin equations of motion.

Examples are mesoscopic dust particles in plasmas (so-called “complex plasma”)¹⁰. Pairs of such dust particles can be brought into a joint self-propulsion¹¹ by non-reciprocal interactions induced by ionic wake charges¹². These motions are only virtually damped. Another important realization are granulates made self-propelling on a vibrating plate^{13–22} or equipped with an internal vibration motor²³ where it has been shown that the active Langevin model indeed describes their dynamics well^{24–26}. Further examples for self-propelled particles with inertia range from mini-robots^{27,28} to macroscopic swimmers like beetles flying at water interfaces²⁹ and whirling fruits self-propelling in air³⁰.

In this perspective article, we first briefly review basic features and predictions of active Brownian motion discussing both swimmers moving on average on a straight line (“linear swimmers”) and particles swimming on a circle (“circle swimmers”). Both single particle properties and collective effects such as motility-induced phase separation are briefly discussed. We then extend the model towards active Langevin motion including inertia and summarize recent developments. We show that some of the basic properties of active Brownian motion are qualitatively changed due to inertia. In particular we discuss inertial delay effects between particle velocity and self-propulsion direction, the tuning of the long-time

self-diffusion by the moment of inertia, effect of fictitious forces in non-inertial frames, and the influence of inertia on motility-induced phase separation (MIPS). MIPS is strongly influenced and suppressed by inertia and if there are two coexisting phases of high and low particle density, these coexisting phases possess different kinetic temperatures.

The paper is organized as follows: in section II, we first recapitulate the basic features of active Brownian motion both for linear swimmers and for circle swimmers. Then, in section III, we propose and discuss the model of active Langevin motion

II. ACTIVE BROWNIAN MOTION FOR SELF-PROPELLED COLLOIDAL PARTICLES (“MICROSWIMMERS”)

Let us first recapitulate the basic features for overdamped active Brownian motion. In the xy -plane, a single particle trajectory at time t is described by the particle center $\vec{r}(t) = (x(t), y(t))$ and particle orientation $\hat{n}(t) = (\cos \phi(t), \sin \phi(t))$ where $\phi(t)$ is the angle of the particle orientation with the x -axis. We now distinguish between linear swimmers and circle swimmers which experience a systematic torque and exhibit chirality.

A. Linear swimmers

For linear swimmers, the basic overdamped equations of motion read as

$$\gamma \dot{\vec{r}}(t) = \gamma v_0 \hat{n}(t) + \vec{f}(t) \quad (1)$$

$$\gamma_R \dot{\phi} = g(t) \quad (2)$$

These equations couple translational and rotational motion and represent a force and torque balance. In detail, γ denotes a translational friction coefficient, v_0 is the imposed self-propulsion speed of the active particle and γ_R is a rotational friction coefficient. The components of $\vec{f}(t)$ and $g(t)$ are Gaussian random numbers with zero mean and variances representing white noise from the surrounding, i.e. $\overline{f(t)} = 0$, $\overline{f_i(t)f_j(t')} = 2k_B T \gamma \delta_{ij} \delta(t-t')$, $\overline{g(t)} = 0$, $\overline{g(t)g(t')} = 2k_B T \gamma_R \delta(t-t')$ where the overbar means a noise average. Here $k_B T$ denotes an effective thermal energy quantifying the translational noise strength. Likewise $k_B T_R$ characterizes the orientational noise strength. In many applications, these temperatures are set to be equal, i.e. $T \equiv T_R$, in others the translational noise is neglected with respect to the rotational noise such that $T = 0$ and $T_R > 0$. In the noise-free case $T = T_R = 0$, the self-propelled motion is linear along the particle orientation, i.e. the self-propelled particle is a *linear swimmer*. Its propulsion

speed is the imposed v_0 . As a remark, the orientational dynamics can equivalently be written as

$$\gamma_R \dot{\hat{n}} = \vec{g}(t) \times \hat{n} \quad (3)$$

where we extended all vectors to three dimensions such that $\hat{n} = (n_x, n_y, 0)$ and $\vec{g}(t) = (0, 0, g(t))$.

Let us first discuss the number of independent parameters inherent in the equations of motion (1) and (2) in the steady state. By choosing suitable units for length and time such as the persistent length $\ell_p = v_0/D_r$ and the persistence time $\tau_p = 1/D_r$ where $D_r = k_B T_R/\gamma_R$ denotes the rotational diffusion constant, a scaling of the equations results in only one remaining independent parameter which can be chosen to be a dimensionless *Peclet number*

$$Pe = \gamma v_0 \sqrt{\gamma \gamma_R / k_B^2 T T_R} \quad (4)$$

This Peclet number measures the strength of activity with respect to noise, it diverges for the zero translational noise such that in this case the model set by Eqns. (1) and (2) is a completely parameter-free persistent random walk solely characterized by the persistence length and persistence time.

We now address the noise-averaged displacement as a function of time t for a prescribed initial orientation $\hat{n}(0)$ at time $t = 0$. It is given by^{4,31}

$$\overline{\vec{r}(t) - \vec{r}(0)} = \frac{v_0}{D_r} (1 - e^{-D_r t}) \hat{n}(0) = \ell_p (1 - e^{-t/\tau_p}) \hat{n}(0) \quad (5)$$

This represents a linear segment oriented along $\hat{n}(0)$ whose total length is the persistence length. The intuitive interpretation of Eq. (5) is that due to the coupling between translational and rotational motion the trajectories show a persistence, it is a persistent random walk rather than a standard random walk. The particle remembers where it came from since it is self-propelled along its orientation and the orientation diffuses with D_r . It is the orientational fluctuations which are governing the persistence not the translational fluctuations. The motion is therefore a “random drive” rather than a “random walk”: A blind driver steers a car with fluctuations in the steering wheel orientation, and this is what makes the motion persistent.

Next we can calculate the mean-square displacement (MSD) which is analytically given by^{4,31}:

$$\overline{(\vec{r}(t) - \vec{r}(0))^2} = \frac{v_0^2}{D_r^2} (D_r t - 1 + e^{-D_r t}) + 4Dt \quad (6)$$

Of course it does not depend on the initial orientation $\hat{n}(0)$ due to symmetry. Expanding Eq. (6) for small, intermediate and long times, we obtain the diffusive short-time limit for the MSD as $4Dt$ where D is the translational short-time diffusion which can be expressed as $D = \ell_p^2/\tau_p Pe$. The initial diffusive regime is then followed by a ballistic regime at intermediate times where the MSD scales roughly as $(v_0 t)^2$. For long times, the

MSD is again diffusive but with a much larger long-time diffusion coefficient

$$D_L = \lim_{t \rightarrow \infty} \frac{1}{4t} \overline{(\vec{r}(t) - \vec{r}(0))^2} = D + v_0^2/4D_r = (1/Pe + \frac{1}{4})\ell_p^2/\tau_p \quad (7)$$

Remarkably, for strong self-propulsion, D_L is much larger than D (i.e. $Pe \rightarrow \infty$) such that $D_L = \ell_p^2/\tau_p$ consistent with the persistent random walk picture.

It is important to note that in the overdamped Brownian model the velocities $\vec{r}(t)$ are not real observables as they fluctuate without any bounds due to the noise terms in Eq. (1). Instead can define an averaged or drift velocity by $\vec{v}_d(t) = \lim_{\Delta t \rightarrow 0} (\vec{r}(t + \Delta t) - \vec{r}(t))/\Delta t$ which is given $\vec{v}_d(t) = v_0 \hat{n}(t)$, i.e. the systematic part of the particle drift velocity is the self-propulsion velocity. However, still one can define a velocity autocorrelation function $Z(t)$ as a second time-derivative of the mean-square displacement³²

$$Z(t) = \frac{d^2}{dt^2} \overline{(\vec{r}(t) - \vec{r}(0))^2} \quad (8)$$

In the case of active Brownian motion Eq. (6) yields that the velocity autocorrelation function is a *single exponential*

$$Z(t) = v_0^2 \exp(-D_r t) \quad (9)$$

decaying with the persistence time $\tau_p = 1/D_r$. This result also implies that the mean squared velocity is the self-propulsion speed as in the short-time limit $Z(0) = v_0^2$.

Remarkably the orientational correlation function $C(t)$ is also a *single exponential*

$$C(t) = \overline{\hat{n}(t) \cdot \hat{n}(0)} = \exp(-D_r t) \quad (10)$$

decaying with the same persistence time $\tau_p = 1/D_r$, i.e. it is proportional to $Z(t)$. This documents that we have standard Brownian orientational diffusion in two dimensions³³.

Finally one finds for the correlation function between particle orientation and drift velocity the result

$$\begin{aligned} c(t', t) &= \lim_{\Delta t \rightarrow 0} \overline{\hat{n}(t') \cdot (\vec{r}(t + \Delta t) - \vec{r}(t))/\Delta t} \\ &= v_0 \exp(-D_r |t - t'|) \end{aligned} \quad (11)$$

and a delay function which measures how the dynamical changes of orientation and velocities are correlated can be defined via

$$d(t) = c(t, 0) - c(0, t) \equiv 0 \quad (12)$$

The delay function trivially vanishes here by symmetry but this will not hold for inertia as discussed later.

Experimental data for the noise averages obtained for dilute self-propelled colloidal Janus particles could indeed be described with these predictions^{31,34} establishing the active Brownian motion model for active colloidal particles.

B. Circle swimmers

In practice, microswimmers are not perfectly rotational symmetric around their swimming axis. An asymmetry leads to a systematic circular motion or chiral motion. In two spatial dimensions, this has been described by including an effective torque M in the equations of motion³⁵ as

$$\gamma \dot{\vec{r}}(t) = \gamma v_0 \hat{n}(t) + \vec{f}(t) \quad (13)$$

$$\gamma_R \dot{\phi} = M + g(t) \quad (14)$$

The noise-free trajectories are circles with a spinning frequency

$$\omega_s = \frac{M}{\gamma_R} \quad (15)$$

and a spinning radius

$$R_s = \frac{v_0 \gamma_R}{M} \quad (16)$$

The sign of the torque M determines whether the circling motion is clockwise or anti-clockwise. Now compared to Eqns. (1) and (2) there is an additional independent system parameter which can be chosen as an additional reduced time scale related to the spinning frequency $\omega_s \tau_p = \frac{M}{\gamma_R} \tau_p$.

Again the mean displacement can be calculated analytically and turns out to be a logarithmic spiral ("*spira mirabilis*") given by³⁵:

$$\begin{aligned} \overline{\vec{r}(t) - \vec{r}(0)} &= \lambda (D_r \hat{n}(0) + \omega_s \hat{n}^\perp(0) \\ &\quad - e^{-D_r t} (D_r \hat{n} + \omega_s \hat{n}^\perp)) \end{aligned} \quad (17)$$

with $\lambda = v_0/(D_r^2 + \omega_s^2)$

$$\hat{n}^\perp(0) = (-\sin \phi(0), \cos \phi(0))$$

$$\hat{n} = (\cos(\omega_s t + \phi(0)), \sin(\omega_s t + \phi(0))), \text{ and}$$

$$\hat{n}^\perp = (-\sin(\omega_s t + \phi(0)), \cos(\omega_s t + \phi(0)))$$

Likewise the MSD for circle swimmers is obtained as³⁵:

$$\begin{aligned} \overline{(\vec{r}(t) - \vec{r}(0))^2} &= 2\lambda^2 [\omega_s^2 - D_r^2 + D_r(D_r^2 + \omega_s^2)t + e^{-D_r t} \\ &\quad \cdot [(D_r^2 - \omega_s^2) \cos \omega_s t - 2D_r \omega_s \sin \omega_s t]] + 4Dt \end{aligned} \quad (18)$$

which is diffusive for both short times and long times with the short-time diffusion coefficient D and the long-time diffusion coefficient

$$D_L = D + \frac{v_0^2 D_r}{4(D_r^2 + \omega_s^2)} \quad (19)$$

which implies that circular spinning will reduce the long-time diffusion coefficient.

From Eq. (8) the velocity autocorrelation function can be calculated as

$$Z(t) = v_0^2 \cos(\omega_s t) \exp(-D_r t) \quad (20)$$

It is not a single exponential but contains a further time scale $1/\omega_s$ reflecting the systematic spinning of the particle orientation.

Finally the orientational correlation function is

$$C(t) = \overline{\hat{n}(t) \cdot \hat{n}(0)} = \cos(\omega_s t) \exp(-D_r t) \quad (21)$$

It is proportional to $Z(t)$ and contains the further time scale $1/\omega_s$ of particle circling as well.

For anisotropic colloidal self-propelled Janus particles, the active Brownian model was tested in detail. In particular, the *spira mirabilis* for the mean displacement was confirmed⁵.

The active Brownian motion of a single particle can be generalized to the presence of external potentials (such as confinement or gravity) and external flow fields (such as linear shear flow), for a review of the different situations considered, see⁷.

C. Collective effects of active Brownian particles: MIPS

Active Brownian particles exhibits a wealth of fascinating collective effects including swarming¹, clustering^{7,36}, crystallization³⁷⁻⁴⁰ and turbulence⁴¹. Here we focus more on one important effect that is purely induced by activity and is called motility-induced phase separation (MIPS). It was seen in computer simulations of active Brownian particles without aligning interactions^{42,43} and confirmed in experiments on artificial colloidal Janus particles^{43,44}.

The basic idea behind MIPS is as follows: Consider a system of active Brownian particle at a finite concentration where the particle are interacting by purely repulsive non-aligning interactions. Suppose two particles meet in a perfect central collision as sketched in Figure 1a. They will not bounce back but stay close to eachother until rotational diffusion will turn the orientations away such they can pass along eachother. This process will happen on a time scale of $\tau_p = 1/D_r$. If other particles will approach the particle pair within this time, the pair will be surrounded by more particles, a cluster is formed and it will get increasingly difficult to release the particles from the cluster. The cluster is thus growing and ideally there is complete phase separation into a dense region inside the cluster and a dilute region outside. Clearly the travel time from a neighbouring particle to the initial pair is governed by the particle motility v_0 , hence the particle phase separation is purely induced by motility and is therefore called motility-induced phase separation (MIPS). Conversely, in equilibrium (i.e. without motility at $v_0 = 0$), purely repulsive interactions will never lead to fluid-fluid phase separation. Clearly MIPS is also favored by higher particle densities since then particle are closer

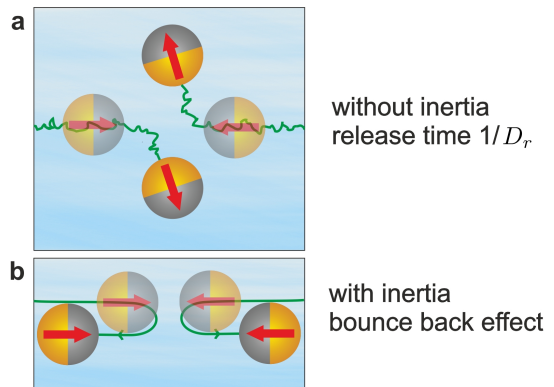


FIG. 1. Sketch of a central elastic collision of two Janus particles with opposing self-propulsion velocities (red arrow): a) active Brownian dynamics: the particles will stay almost touching for a typical time of $1/D_r$. b) active Langevin dynamics: microflyers will bounce back such that they will not exhibit their terminal self-propulsion speed v_0 . Initial positions are shown in light colors. The particle trajectories are rendered in green color.

anyway. In a parameter space spanned by the particle density and the Peclet number there is either a one-phase or a two-phase region. This is by now well-explored by simulation, theory and experiment and there are several reviews on this topic^{7,36,45-48}.

More recently MIPS has also been seen for circle swimmers^{49,50} and more complicated aligning interactions^{51,52}. This shows that the occurrence of MIPS itself is a very robust and general effect. Moreover the growth exponent of the cluster size as a function of time has been simulated⁵³ and studied by theory⁵⁴. At the late stage, for long times, a universal power law similar to the Cahn-Hilliard theory was found with a universal growth exponent of $1/3$.

III. ACTIVE LANGEVIN MOTION FOR SELF-PROPELLED PARTICLES WITH INERTIA (“MICROFLYERS”)

A. Single particles

We now generalize the equations of active Brownian to that of active Langevin motion including inertia both for the translational and the rotational part, see e.g. Refs.^{23,26,55-64}, as

$$\begin{aligned} m\ddot{\vec{r}} + \gamma(\dot{\vec{r}}) &= \gamma v_0 \hat{n} + \vec{f}(t) \\ J\ddot{\phi} + \gamma_R \dot{\phi} &= M + g(t) \end{aligned} \quad (22)$$

Here, m is the particle mass and J the moment of inertia. In case the orientational relaxation is fast, one may consider the limit of vanishing moment of inertia, $J = 0$ ^{56-58,61}. For $M = 0$ we recover active Langevin motion for linear microflyers, for $M \neq 0$ these are circle

flyers. Now the particle velocity and the orientation are not necessarily proportional.

On top of the parameters characterizing a Brownian circle swimmer discussed in II B, there are now two more system parameters. These can be best put in terms of two additional relaxation times scales due to finite moment of inertia and mass. The *orientational relaxation time* upon which an angular velocity relaxes due to the finite moment of inertia is given by

$$\tau_r = J/\gamma_R \quad (23)$$

In case the orientational relaxation is fast, $\tau_r \rightarrow 0$, one may consider the limit of vanishing moment of inertia, $J = 0$ which was assumed in several recent studies^{56–58,61}. Correspondingly there is also a second time, the *translational relaxation time*,

$$\tau = m/\gamma \quad (24)$$

upon which the translational velocities relax due to the finite mass m .

With suitable basic length and time scales of the persistence random walk, ℓ_p and τ_p , we can state the four independent system parameters of Eq. (22) as three basic dimensionless *delay numbers* $\mathcal{D}_0 = \tau_r/\tau_p$, $\mathcal{D}_1 = \omega_s \tau_r$, $\mathcal{D}_2 = \tau_r/\tau$ plus the Peclet number Pe defined in Eq. (4) which contributes a time scale for the translational Brownian motion.

Some analytical solutions of the active Langevin motion model are given in Ref.²⁶ which we briefly review here. There is an analytical result for the noise-averaged and time-resolved displacements and mean-square-displacements⁶⁵. Four different regimes can be identified where the MSD exhibits different power laws: ballistic for very short times, then diffusive due to solvent noise, then ballistic again due to self-propulsion and then diffusive again for very long times due to randomizing particle orientation. The long-time translational self-diffusion coefficient D_L can be calculated as

$$D_L = D + \frac{v_0^2}{2} \mathfrak{t}(\tau_r, \mathcal{D}_0, \mathcal{D}_1) \quad (25)$$

This equations has a similar structure than the result for overdamped dynamics, see Eq. (7), insofar that is a superposition of the translational diffusion and an active term proportional to v_0^2 . The corresponding time scale is given by

$$\mathfrak{t}(\tau_r, \mathcal{D}_0, \mathcal{D}_1) = \tau_r e^{\mathcal{D}_0} \text{Re} \left[\mathfrak{D}_0^{-(\mathcal{D}_0 - i\mathcal{D}_1)} \gamma(\mathcal{D}_0 - i\mathcal{D}_1, \mathcal{D}_0) \right] \quad (26)$$

where Re denotes the real part and $\gamma(y, z)$ is the lower incomplete gamma function. Interestingly, the time scale (26) does *not* depend on the translational relaxation time τ but it depends explicitly on the rotational relaxation time τ_r . This is in contrast to equilibrium ($v_0 = 0$) where

D_L neither depends on τ nor on τ_r . In fact, the dependence of long-time diffusion on the moment of inertia is pretty strong as

$$D_L = D + v_0^2 \sqrt{\frac{\pi}{8D_r \xi_r}} \sqrt{J} + \mathcal{O}(\sqrt{J^{-1}}) \quad (27)$$

As an application animals can hardly change mass but they can change their moment of inertia during motion. So this may provide a strategy to sample space more quickly.

Moreover the zero-time velocity correlation, i.e. the mean kinetic energy, can be calculated as

$$\overline{\dot{r}^2} = 2D/\tau + \mathfrak{f}(\mathcal{D}_0, \mathcal{D}_1, \mathcal{D}_2) v_0^2 \quad (28)$$

with

$$\mathfrak{f}(\mathcal{D}_0, \mathcal{D}_1, \mathcal{D}_2) = \mathfrak{D}_2 e^{\mathcal{D}_0} \text{Re} \left[\mathfrak{D}_0^{-(\mathcal{D}_0 - i\mathcal{D}_1 + \mathcal{D}_2)} \times \gamma(\mathcal{D}_0 - i\mathcal{D}_1 + \mathcal{D}_2, \mathcal{D}_0) \right] \quad (29)$$

The first term in (28) is the equilibrium solution for a passive particle ($v_0 = 0$) and the second arises from the active motion. The latter is proportional to v_0^2 , i.e. the kinetic energy injected by the propulsion.

Remarkably the orientational correlation function $C(t)$ is a *double exponential*

$$C(t) = \overline{\hat{n}(t) \cdot \hat{n}(0)} = \cos \omega_s t \exp(-D_r(t - \tau_r(1 - e^{-t/\tau_r}))) \quad (30)$$

emphasizing again the important role of rotational inertial relaxation since the time scale τ_r enters here explicitly.

Finally one finds for the delay function which measures how the dynamical changes of orientation and velocities are correlated

$$\begin{aligned} \overline{\dot{r}(t) \cdot \hat{n}(0)} - \overline{\dot{r}(0) \cdot \hat{n}(t)} &= v_0 \mathfrak{D}_2 e^{\mathcal{D}_0} \mathfrak{D}_0^{(\mathcal{D}_2 - \mathcal{D}_0)} e^{-t/\tau} \\ &\times \text{Re} \left[\mathfrak{D}_0^{i\mathcal{D}_1} \left(\mathfrak{D}_0^{-2\mathcal{D}_2} \gamma(\mathcal{D}_0 - i\mathcal{D}_1 + \mathcal{D}_2, \mathcal{D}_0) \right. \right. \\ &\quad \left. \left. - e^{2t/\tau} \mathfrak{D}_0^{-2\mathcal{D}_2} \gamma(\mathcal{D}_0 - i\mathcal{D}_1 + \mathcal{D}_2, \mathcal{D}_0) e^{-t/\tau_r} \right. \right. \\ &\quad \left. \left. - \gamma(\mathcal{D}_0 - i\mathcal{D}_1 - \mathcal{D}_2, \mathcal{D}_0) e^{-t/\tau_r} \right. \right. \\ &\quad \left. \left. + \gamma(\mathcal{D}_0 - i\mathcal{D}_1 - \mathcal{D}_2, \mathcal{D}_0) \right) \right]. \end{aligned} \quad (31)$$

By definition, this function is zero for $t = 0$ and is then strictly positive exhibiting a maximum after a typical characteristic delay time. This shows that on average first the particle orientation will change and then the particle velocity will follow on the scale of this delay time.

We close this section with two remarks: First, for $J = 0$ there is an equivalence to overdamped particle motion in a harmonic potential as can easily be seen by replacing the role of velocities and positions in the equations of motion. This mapping has lead to some other exact results

for the dynamics obtained by Malakar and coworkers⁶⁶. Second, there are more complicated models to describe an additional alignment between particle orientation and velocity which is ignored in Eq. (22). This seems to be a more realistic description of granular hoppers^{23,67} but lacks an analytical solution. It has been applied to inertial active particles in a harmonic external potential recently²³. This extra term involves an additional torque such that the orientational dynamics in Eq. (22) can be written for $J = 0$ as

$$\gamma_R \dot{\hat{n}} = \zeta(\hat{n} \times \dot{\vec{r}}) \times \hat{n} + (\vec{M} + \vec{g}(t)) \times \hat{n} \quad (32)$$

where ζ is a coupling coefficient.

B. Self-propulsion of microflyers in non-inertial frames

The equations of motion Eq. (22) can be generalized to non-inertial frames to describe self-propulsion on rotating disks or on oscillating plates, for example, as has been discussed recently⁶⁸. The new phenomenon for active Langevin motion in this set-up is that additional fictitious forces have to be added to the equations of motion if the equations are expressed in the non-inertial frame. We briefly illustrate this for a planar rotating disk and for an oscillating plate.

1. Rotating disk

On a planar disk rotating around the z -axis with a constant angular velocity ω , the equations of motion for a particle self-propelling on the xy -plane read in the laboratory frame as

$$\begin{aligned} m\ddot{\vec{r}} + \gamma(\dot{\vec{r}} - \vec{\omega} \times \vec{r}) &= \gamma v_0 \hat{n} + \vec{f}(t) \\ J\ddot{\phi} + \gamma_R(\dot{\phi} - \omega) &= M + g(t) \end{aligned} \quad (33)$$

The ingredient here is that friction is proportional to the *relative* velocity and the *relative* angular velocity in the rotating non-inertial frame. If expressed as equations of motion in the rotating frame, the friction term is getting easier but additional centrifugal and Coriolis forces need to be included.

In the noise-free case, the solution can be found analytically and is given by a superposition of three terms: two logarithmic spirals which spiral inwards and outwards with different rates and a constant rotation around the rotation origin with radius

$$b = \frac{\gamma v_0}{\sqrt{m^2(\omega + \omega_s)^4 + \gamma^2 \omega_s^2}} \quad (34)$$

The special circular solution can be understood as arising from a balance of the centrifugal force, the self-propulsion force and the friction force in the rotating frame. However, it is unstable with respect to the out-spiraling part

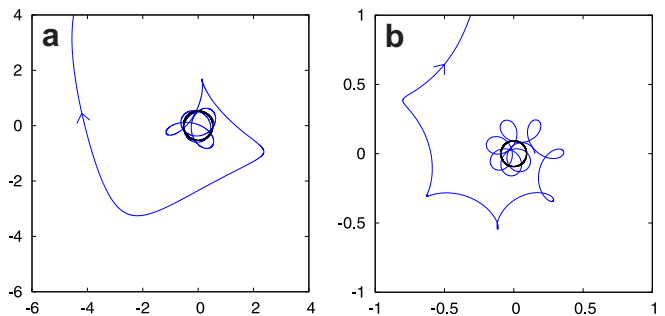


FIG. 2. Typical trajectories from the analytical solution of the noise-free Eq. (33) in the laboratory frame. The unstable rotation with radius b is indicated as a black circle. The trajectory approaches a logarithmic spiral. The length unit is v_0/ω and the parameters are: $\gamma/m\omega = 2.5$ a) $\omega_s/\omega = 1$ and b) $\omega_s/\omega = 4$

which stems from the action of the centrifugal force. The actual trajectories look pretty complex in the laboratory frame. An example is shown in Figure 2. For an overdamped system, these fictitious forces do not exist and a particle does not suffer from the centrifugal expulsion from the rotation center.

2. Oscillating plate

We now consider active Langevin motion on a two-dimensional oscillating plate. The oscillating plate constitutes a linearly accelerated frame of reference as described with a time dependent distance vector

$$\vec{R}_0(t) = D_p \cos(\omega_p t) \vec{e}_x \quad (35)$$

between the origins of the inertial laboratory frame and the non-inertial frame. Here D_p is an oscillation amplitude, ω_p is the oscillation frequency of the plate and the oscillation is taken along the x -axis without loss of generality. The equations of motion in the laboratory frame are

$$m\ddot{\vec{r}} + \gamma(\dot{\vec{r}} - \dot{\vec{R}}_0(t)) = \gamma v_0 \hat{n} + \vec{f}(t) \quad (36)$$

$$\gamma_R \dot{\phi} = M + g(t) \quad (37)$$

and the solution in the noise-free case can be obtained analytically as a superposition of harmonic terms with frequencies ω_p and M/γ_R in x -direction. One term is exponentially damped with rate γ/m , another is persistent and undamped. The effect of noise, the noise-averaged trajectory and the MSD can be calculated analytically following the analysis proposed in⁶⁸. For large ω_p (i.e. $\omega_p \gg M/\gamma_R$) there is an enormous amplification of the oscillation amplitude due to the fictitious centrifugal force.

C. Collective effects: MIPS

Since motility-induced phase separation (MIPS) is in general a pretty robust effect, it is expected to occur also for inertial active particles provided the inertial effects are not too large. In fact, recent studies^{69,70} have explored the active Langevin model in this regard and found that inertia as modelled by the many-body generalization of Eq. (22) is unfavorable for MIPS. An example is shown in Figure 3 where the phase separation separatrix is shown for fixed density in the parameter space spanned by the Peclet number Pe and the particle mass m . In this case, the moment of inertia J and the external torque M were both set to zero. In fact, beyond a critical mass, there is no phase separation at all. Generally speaking this has to do with the additional fluctuations which occur in the active system introduced by inertia. If we take the intuitive picture for MIPS in underdamped systems described in II C, it is now getting different: with inertia, a centrally colliding particle pair will *bounce back* rather than staying static and Brownian as it does in the overdamped case, see Figure 1b. This will destroy the nucleus for subsequent particle aggregation more than it does in the overdamped case and therefore MIPS is unfavored by inertia. Moreover there is a re-entrant one-phase region if the activity (or Peclet number) is increased which is strongly amplified by inertia.

But when MIPS occurs for inertial active particles there is novel effect that does not occur for overdamped systems: the two coexisting phases exhibit a different temperature^{70,71}. Here temperature is defined via the mean kinetic energy of the particles. Figure 4 shows the underlying principle. In contrast to granulates where a similar effect has been found⁷², particle collisions are elastic here but the self-propulsion makes a collision between two particles like two bouncing balls hitting each other, see again Figure 1b. Thus particles will never possess a velocity along their orientation when there are many subsequent inter-particle collisions. Therefore the dense region is "cool" (in terms of kinetic temperature) while in the dilute region particles will accelerate until they have almost reached their terminal velocity v_0 . Hence the dilute region is "hot". The temperature difference between the dilute and dense regions can be huge up to a factor of 100. Note that there is no flux of heat at the fluid-fluid interface but a stable thermal gradient will be established there.

Finally the growth of particle clusters during the phase separation process has been explored by computer simulation⁷⁰. These calculations reveal that the cluster growth exponent is significantly lower than the universal value of $1/3$ found in the overdamped case^{53,54} proving that inertia can qualitatively change the physics of the collective phenomena.

In summary, in the active Langevin model, there are three basic effects which are caused by inertia as far as motility-induced phase separation is concerned: the

phase separation is shifted towards higher Peclet number and is finally destroyed completely as the particle mass is increased. Second, the kinetic temperature is different in the two coexisting phases in stark contrast to equilibrium thermodynamics where phase coexistence implies equality of temperatures. Third, the cluster growth exponents is smaller than the universal value $1/3$ valid for overdamped systems.

IV. SUMMARY OF TRANSLATIONAL AND ORIENTATIONAL DYNAMICAL AUTOCORRELATION FUNCTIONS

In Table I we summarize the different cases discussed so far in terms of the translational and orientational dynamical autocorrelation functions $Z(t)$ and $C(t)$. We distinguish between a simple single exponential decay with one decay time and more complicated behavior such as an oscillatory decay (valid for circle swimmers) or double exponentials (valid for microflyers with $M = 0$ and $J > 0$). The passive cases are listed as references. For passive Langevin dynamics

$$m\ddot{\vec{r}}(t) + \gamma\dot{\vec{r}}(t) = \vec{f}(t) \quad (38)$$

with $\vec{f}(t)$ denoting white Gaussian noise, the velocity autocorrelation function $Z(t)$ decays as a simple exponential with a decay time m/γ and the orientational dynamics is decoupled from this equation. For $J = 0$ and $M = 0$, the orientational correlation is single exponential, but not for $J > 0$ where it is a double exponential or for $M > 0$ where it is oscillatory.

For many particles with non-aligning interactions (at vanishing external torque, $M = 0$), the orientational correlation function is still a single exponential, but the translational correlation function is highly nontrivial (even for passive particles³²) while for aligning interactions also the orientational dynamics is complicated³³.

V. EXPERIMENTAL REALIZATION

A. General

Inertial effects are getting relevant in particular for two different situations: i) for *macroscopic* self-propelled particles, ii) for mesoscopic particles on the colloidal scale moving in a medium of *low viscosity* (such as a gas).

Regarding the first situation, one of the best realization of our model equations (22) for active Langevin dynamics can be found for active granulates¹³⁻²². Typically these are hoppers with a Janus-like body or with tilted legs. In order to achieve self-propulsion, these macroscopic bodies are either placed on a vibrating table or are equipped with an internal vibration motor ("hexbugs")²³. It has been shown that the dynamics of these hoppers is well described by active Brownian motion with inertia²⁴⁻²⁶.

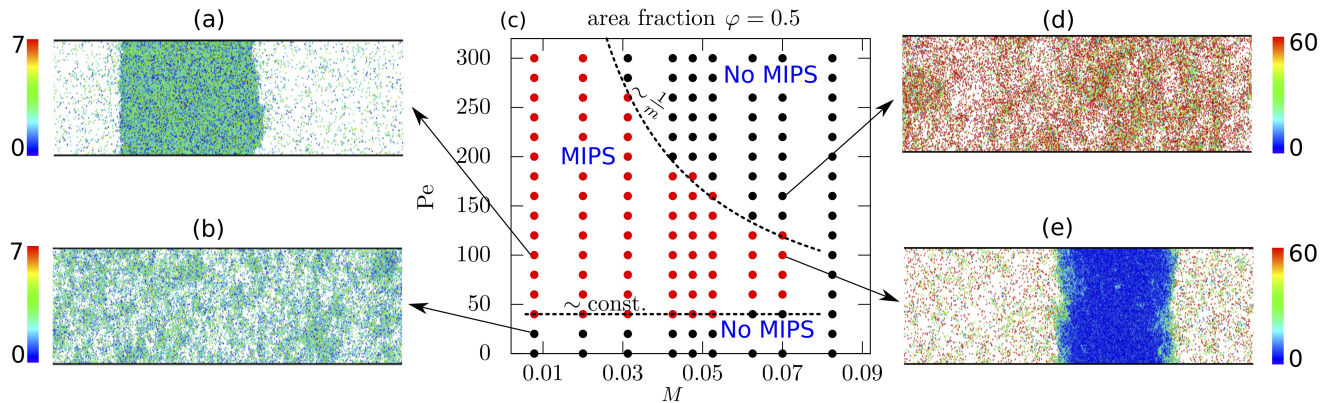


FIG. 3. Nonequilibrium phase diagram at an area fraction of $\phi = 0.5$ in the plane spanned by the particle mass and the self-propulsion speed (arbitrary units) (c). Panels (a), (b), (d), and (e) represent simulation snapshots in slab geometry at state points indicated in the phase diagram. Colors represent kinetic energies of individual particles in units of $k_B T$. A hot-cold coexistence is visible in panel (e). Dashed lines in (c) show scaling predictions for the phase boundary between the homogeneous and phase-separated state. From Ref.⁷⁰.

	translational velocity correlation $Z(t)$		orientational correlation $C(t)$	
	single exponential	more complicated	single exponential	more complicated
single particle				
passive Brownian motion	X		X	
active Brownian motion	X		X	
Brownian circle swimmer		X		X
passive Langevin ($J = M = 0$)	X		X	
passive Langevin ($J > 0$ or $M > 0$)	X			X
active Langevin ($M = J = 0$)		X	X	
active Langevin ($J \neq 0$)		X		X
many interacting particles				
non-aligning ($M = 0$)		X	X	
aligning interaction		X		X

TABLE I. Summary of the behavior of translational and orientational correlation functions $Z(t)$ and $C(t)$ for different situations of single and many passive and active particles. In particular a simple single exponential decay is indicated. All four different combinations do occur, the models belonging to the corresponding classes are listed.

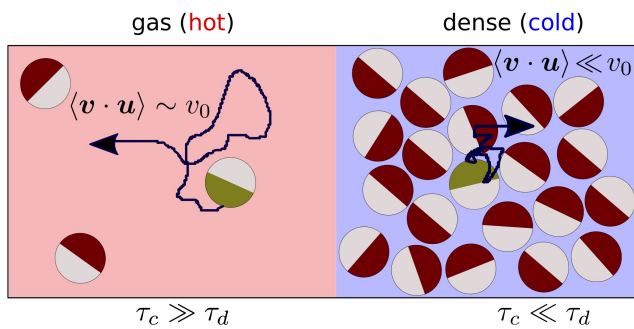


FIG. 4. Scheme of the phase-separated state associated with a hot-cold coexistence in underdamped active particles. Particles self-propel with the colored cap ahead (brown; greenish for the tagged particle). Active particles move with v_0 in the gas phase, but can be an order of magnitude slower in the dense phase. From Ref.⁷⁰.

Since they are macroscopic, inertia is relevant. The fluctuations can be fitted to Brownian forces and imperfections in the particle symmetry will make them circling ($M \neq 0$). Therefore, they are ideal realizations of our model equations (22) but there is a caveat for certain granulates insofar as the additional aligning torque described in Eq. (32) needs to be included. Moreover, there is no major difficulty in placing granulates on a turntable or on an oscillating plate so that effects arising from a non-inertial frame are directly accessible. There is a plethora of other examples of macroscopic self-propelling objects which are dominated by inertia. These include mini-robots^{27,28}, flying whirling fruits²⁶ as well as cars, boats, airplanes, swimming and flying animals³⁰ and moving pedestrians, bicyclists and vehicles^{73–75}.

Regarding the second situation, dust particles in plasmas (“complex plasmas”) can be made active⁷⁶. They exhibit underdamped dynamics due to the presence of the neutral gas¹⁰ and are therefore highly inertial. Another example in nature are fairyflies which belong to

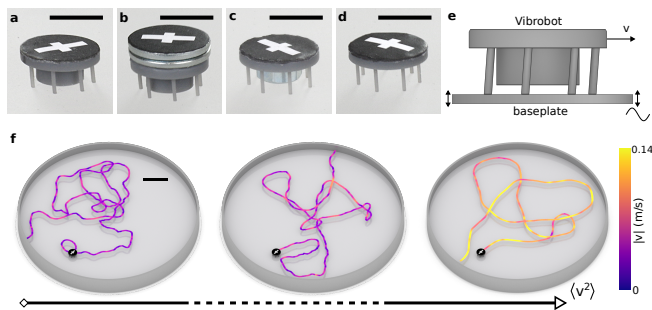


FIG. 5. **3D printed particles, setup and trajectories.** **a** Generic particle **b** Carrier particle with an additional outer mass. **c** Tug particle with an additional central mass. **d** Ring particle without a central core. **e** Illustration of the mechanism with a generic particle on a vibrating plate. **f** Three exemplary trajectories with increasing average particle velocities. Particle images mark the starting point of each trajectory. The trajectory colour indicates the magnitude of the velocity. From Ref.²⁶.

the smallest flying insects on our globe and have a size of several hundreds of microns.

B. Vibrated granulates in particular

As already mentioned, a direct realization of active Langevin motion is obtained for vibrated granulates. Interestingly, particles can be prepared with different mass and different moments of inertia, see Ref.²⁶ which we describe now in more detail. Exposed to a vibrating plate, they perform self-propulsion in two dimensions, see Figure 5 for the experimental realization and typical particle trajectories. The actual particle velocity along the trajectories is not constant but fluctuates and the mean-square displacements and orientational correlations are in good agreement with the active Langevin model when some parameters are fitted to the experiments. In particular, the velocity distribution function has a peak around the self-propulsion velocity.

Interestingly experimental data for the inertial delay as embodied in the delay correlation function $d(t)$ (see Eq. (31)) are both in qualitative and quantitative agreement with the theoretical result. An example is shown in Figure 6. Indeed the theoretical prediction is confirmed by the experimental data averaged over the noise. This documents that first the direction of self-propulsion is changed and the velocity follows. As this delay effect is missing in the overdamped case, it is caused completely by inertia. It is exactly this inertial delay effect which is used by oversteering racing cars to get around corners. We finally remark that, as compared to hexbugs, no self-aligning forces²³ need to be incorporated to get a reasonable fit of the data.

VI. PERSPECTIVES

In the flourishing field of active matter most of the previous investigations used simple overdamped dynamics such as active Brownian motion to model microswimmers and meso-scale self-propelled colloids. If it comes to more macroscopic active particles (granulates or microbots) or to motion in a gas (“microflyers”), inertial effects become relevant. Therefore it is expected that future research will include more and more aspects of inertia also on a more fundamental level. In this article we have mainly touched the basic model description of inertial active matter and their realization in granulate experiments.

Future activities and promising perspectives are expected along the following directions:

First, granulate particles will play a leading role as *paradigmatic realizations* for active matter models. Since they are macroscopic, the particles can more easily be manipulated and changed. The particle shape can be easily changed by macroscopic 3d-printing and different particle interactions can be established. In detail:

i) The whole field of *charged active matter* which unifies strongly coupled unscreened Coulomb systems⁷⁷ and active matter can be realized by charging granulates, either by tribo-electric effects and by preparing macroscopic charged particles⁷⁸. This is possibly a better controlled charged system than that of charged active dusty plasmas which require nonequilibrium ionic fluxes.

ii) Dipolar active particles with permanent magnetic dipole moments are not easy to synthesize on the colloidal level^{79–82} but can directly be realized by equipping granulates with little permanent magnets.

iii) We are just at the beginning to study active polymers as colloidal chains. While there is an increasing number of simulation and theoretical studies, see⁸³ for a recent review, experimental studies with active polymers and colloidal chains in an active bath are sparse⁸⁴. The effect of inertial dynamics on active polymers needs to be understood better and future experiments and simulations are expected in this direction.

iv) It would be highly interesting to study *active surfactants*, to couple the field of surfactants with active matter. Chain-like vibrated granulates with a head and tail part composed of rotators with a different rotation sense⁸⁵ can be prepared and brought into motion to explore the dynamics at a surfactant interface.

v) Studying granulates on a vibrating *structured substrate* will induce anisotropic active motion which has not yet been studied by theory either.

vi) Time-dependent propulsion strengths when the propulsion velocity depends explicitly on time can be realized by granulates, for example by modulating the shaking amplitude on demand. For overdamped systems, some analytical results were obtained for time-dependent propulsions⁸⁶ but inertia is expected to induce new lag-effects in the dynamics.

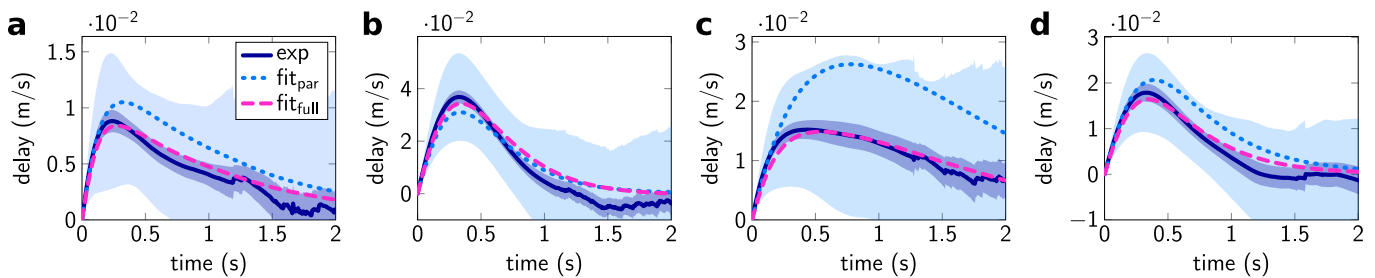


FIG. 6. Delay functions $d(t)$ for the **a** generic, **b** carrier, **c** tug and **d** ring particle. The solid dark blue shows experimental data, the dashed magenta and dotted light blue curve plot theoretical results, with a different way of fitting. Experimental uncertainties are expressed as the standard deviation in light or dark blue regions. From Ref.²⁶.

Second, the motion of inertial active particles will be explored in various *confining geometries* (harmonic trap, confining walls). It has already been shown that in a simple harmonic confinement there are novel dynamical effects²³. This will be even more complex for more complicated confinements.

Third, *collective effects* of active Langevin dynamics needs to be explored more. More studies on MIPS including a non-vanishing moment of inertia and an external torque will be performed. The role of aligning interactions needs to be understood better for inertial systems^{87,88}. Active crystallization will be studied where inertia provides a latent heat upon crystallization. Here we do not only need benchmarking experiments but also fundamental theory including the Langevin dynamics. First attempts in terms of theory have been done by generalizing the swim pressure to the inertial case⁵⁷ and to consider inertial terms in hydrodynamic approaches^{60,89} but certainly also microscopic approaches such as mode-coupling theory^{90,91} and dynamical density functional theory⁹² need to be extended to include inertia. Next, active particles with inertia may provide little heat engines with a better efficiency than their overdamped counterparts as energy is not damped away by the dynamics. We are just at the beginning to understand the principles of entropy production^{93,94} and heat conversion⁹⁵⁻⁹⁷ in these systems.

Finally, inertia introduces some kind of *memory* to the particle motion, both for translational and orientational motion, on the time scale of the inertial relaxation times τ and τ_r . This is the prime reason for delay effects relative to overdamped active Brownian particles. There is a need to classify memory effects in general and to study whether or not the behavior is similar to that in other system governed by memory⁹⁸. One other example where memory effects are crucial is an active particle in a viscoelastic (non-Newtonian) fluid such as a polymer solution⁹⁹ or a nematic liquid crystal^{100,101} where a notable increase of the rotational diffusion coefficient has been found¹⁰². Another example is a sensorial delay in the perception of artificial minirobot systems^{27,28,103} which was shown to have a significant effect on the clustering and swarming properties.

VII. CONCLUSIONS

In conclusion we have upgraded the standard model of active Brownian motion by including inertia in both translational and orientational motion leading to the basic model of active Langevin motion. We discussed single particle properties by the orientational and translational correlation functions presenting some analytical results for this model. When comparing the model to experiments on vibrated granulates, good agreement was found. We summarized some effects induced by inertia including an inertial delay between self-propulsion direction and particle velocity, the tuning of the long-time self-diffusion by the moment of inertia, the effect of fictitious forces in non-inertial frames, and the influence of inertia on motility-induced phase separation. Since inertial effects will necessarily become relevant for length scales between macroscopic and mesoscopic both for artificial self-propelled objects and for living creatures, a booming future of inertial active systems is lying ahead.

ACKNOWLEDGMENTS

I thank Soudeh Jahanshahi, Christian Scholz, Thomas Franosch, Thomas Voigtmann, Alexander Sprenger, Alexei V. Ivlev, Frederik Hauke and Suvendu Mandal for helpful discussions and gratefully acknowledge support by the Deutsche Forschungsgemeinschaft (DFG) through grant LO 418/23-1.

- ¹T. Vicsek, A. Czirók, E. Ben-Jacob, I. Cohen, and O. Shochet, "Novel type of phase transition in a system of self-driven particles," *Phys. Rev. Lett.* **75**, 1226 (1995).
- ²J. R. Howse, R. A. Jones, A. J. Ryan, T. Gough, R. Vafabakhsh, and R. Golestanian, "Self-motile colloidal particles: from directed propulsion to random walk," *Phys. Rev. Lett.* **99**, 048102 (2007).
- ³B. ten Hagen, S. van Teeffelen, and H. Löwen, "Non-gaussian behaviour of a self-propelled particle on a substrate," *Condens. Matter Phys.* **12**, 725-738 (2009).
- ⁴B. ten Hagen, S. van Teeffelen, and H. Löwen, "Brownian motion of a self-propelled particle," *J. Phys.: Condens. Matter* **23**, 194119 (2011).
- ⁵F. Kümmel, B. ten Hagen, R. Wittkowski, I. Buttinoni, R. Eichhorn, G. Volpe, H. Löwen, and C. Bechinger, "Circular motion

- of asymmetric self-propelling particles,” *Phys. Rev. Lett.* **110**, 198302 (2013).
- ⁶C. Kurzthaler, C. Devailly, J. Arlt, T. Franosch, W. C. Poon, V. A. Martinez, and A. T. Brown, “Probing the spatiotemporal dynamics of catalytic janus particles with single-particle tracking and differential dynamic microscopy,” *Phys. Rev. Lett.* **121**, 078001 (2018).
- ⁷C. Bechinger, R. Di Leonardo, H. Löwen, C. Reichhardt, G. Volpe, and G. Volpe, “Active particles in complex and crowded environments,” *Rev. Mod. Phys.* **88**, 045006 (2016).
- ⁸A. Fiasconaro, W. Ebeling, and E. Gudowska-Nowak, “Active brownian motion models and applications to ratchets,” *Eur. Phys. J. B* **65**, 403–414 (2008).
- ⁹P. Romanczuk, M. Bär, W. Ebeling, B. Lindner, and L. Schimansky-Geier, “Active brownian particles-from individual to collective stochastic dynamics p.” *The European Physical Journal Special Topics* **202** (2012).
- ¹⁰G. E. Morfill and A. V. Ivlev, “Complex plasmas: An interdisciplinary research field,” *Rev. Mod. Phys.* **81**, 1353 (2009).
- ¹¹J. Bartnick, A. Kaiser, H. Löwen, and A. V. Ivlev, “Emerging activity in bilayered dispersions with wake-mediated interactions,” *J. Chem. Phys.* **144**, 224901 (2016).
- ¹²A. Ivlev, J. Bartnick, M. Heinen, C.-R. Du, V. Nosenko, and H. Löwen, “Statistical mechanics where newtons third law is broken,” *Phys. Rev. X* **5**, 011035 (2015).
- ¹³V. Narayan, S. Ramaswamy, and N. Menon, “Long-lived giant number fluctuations in a swarming granular nematic,” *Science* **317**, 105–108 (2007).
- ¹⁴C. A. Weber, T. Hanke, J. Deseigne, S. Léonard, O. Dauchot, E. Frey, and H. Chaté, “Long-range ordering of vibrated polar disks,” *Phys. Rev. Lett.* **110**, 208001 (2013).
- ¹⁵C. Scholz, M. Engel, and T. Pöschel, “Rotating robots move collectively and self-organize,” *Nature Commun.* **9**, 931 (2018).
- ¹⁶A. Deblais, T. Barois, T. Guerin, P.-H. Delville, R. Vaudaine, J. S. Lintuvuori, J.-F. Boudet, J.-C. Baret, and H. Kellay, “Boundaries control collective dynamics of inertial self-propelled robots,” *Phys. Rev. Lett.* **120**, 188002 (2018).
- ¹⁷A. Kudrolli, G. Lumay, D. Volfson, and L. S. Tsimring, “Swarming and swirling in self-propelled polar granular rods,” *Phys. Rev. Lett.* **100**, 058001 (2008).
- ¹⁸J. Deseigne, O. Dauchot, and H. Chaté, “Collective motion of vibrated polar disks,” *Phys. Rev. Lett.* **105**, 098001 (2010).
- ¹⁹G. A. Patterson, P. I. Fierens, F. S. Jimka, P. König, A. Garcimartín, I. Zuriguel, L. A. Pugnali, and D. R. Parisi, “Clogging transition of vibration-driven vehicles passing through constrictions,” *Phys. Rev. Lett.* **119**, 248301 (2017).
- ²⁰G. Junot, G. Briand, R. Ledesma-Alonso, and O. Dauchot, “Active versus passive hard disks against a membrane: mechanical pressure and instability,” *Phys. Rev. Lett.* **119**, 028002 (2017).
- ²¹G. Notomista, S. Mayya, A. Mazumdar, S. Hutchinson, and M. Egerstedt, “A study of a class of vibration-driven robots: Modeling, analysis, control and design of the brushbot,” arXiv:1902.10830 (2019).
- ²²S. Mayya, G. Notomista, D. Shell, S. Hutchinson, and M. Egerstedt, “Achieving non-uniform densities in vibration driven robot swarms using phase separation theory,” arXiv:1902.10662 (2019).
- ²³O. Dauchot and V. Démery, “Dynamics of a self-propelled particle in a harmonic trap,” *Phys. Rev. Lett.* **122**, 068002 (2019).
- ²⁴L. Walsh, C. G. Wagner, S. Schlossberg, C. Olson, A. Baskaran, and N. Menon, “Noise and diffusion of a vibrated self-propelled granular particle,” *Soft Matter* **13**, 8964–8968 (2017).
- ²⁵Y. Lanoiselée, G. Briand, O. Dauchot, and D. S. Grebenkov, “Statistical analysis of random trajectories of vibrated disks: towards a macroscopic realization of brownian motion,” *Phys. Rev. E* **98**, 062112 (2018).
- ²⁶C. Scholz, S. Jahanshahi, A. Ldov, and H. Löwen, “Inertial delay of self-propelled particles,” *Nature Commun.* **9**, 5156 (2018).
- ²⁷M. Mijalkov and G. Volpe, “Sorting of chiral microswimmers,” *Soft Matter* **9**, 6376–6381 (2013).
- ²⁸M. Leyman, F. Ogemark, J. Wehr, and G. Volpe, “Tuning phototactic robots with sensorial delays,” *Phys. Rev. E* **98**, 052606 (2018).
- ²⁹H. Mukundarajan, T. C. Bardon, D. H. Kim, and M. Prakash, “Surface tension dominates insect flight on fluid interfaces,” *J. Exp. Biol.* **219**, 752–766 (2016).
- ³⁰J. Rabault, R. A. Fauli, and A. Carlson, “Curving to fly: Synthetic adaptation unveils optimal flight performance of whirling fruits,” *Phys. Rev. Lett.* **122**, 024501 (2019).
- ³¹J. R. Howse, R. A. L. Jones, A. J. Ryan, T. Gough, R. Vafabakhsh, and R. Golestanian, “Self-motile colloidal particles: From directed propulsion to random walk,” *Phys. Rev. Lett.* **99**, 048102 (2007).
- ³²J.-P. Hansen and I. R. McDonald, *Theory of Simple Liquids* (Elsevier, 1990).
- ³³J. K. Dhont, *An Introduction to Dynamics of Colloids*, Vol. 2 (Elsevier, 1996).
- ³⁴X. Zheng, B. ten Hagen, A. Kaiser, M. Wu, H. Cui, Z. Silberli, and H. Löwen, “Non-gaussian statistics for the motion of self-propelled janus particles: Experiment versus theory,” *Phys. Rev. E* **88**, 032304 (2013).
- ³⁵S. van Teeffelen and H. Löwen, “Dynamics of a brownian circle swimmer,” *Phys. Rev. E* **78**, 020101 (2008).
- ³⁶A. Zöttl and H. Stark, “Emergent behavior in active colloids,” *J. Phys. Condens. Matter* **28**, 253001 (2016).
- ³⁷J. Bialké, T. Speck, and H. Löwen, “Crystallization in a dense suspension of self-propelled particles,” *Phys. Rev. Lett.* **108**, 168301 (2012).
- ³⁸P. Digregorio, D. Levis, A. Suma, L. F. Cugliandolo, G. Gonnella, and I. Pagonabarraga, “Full phase diagram of active brownian disks: From melting to motility-induced phase separation,” *Phys. Rev. Lett.* **121**, 098003 (2018).
- ³⁹J. U. Klamser, S. C. Kapfer, and W. Krauth, “Thermodynamic phases in two-dimensional active matter,” *Nature Commun.* **9**, 5045 (2018).
- ⁴⁰J. U. Klamser, S. C. Kapfer, and W. Krauth, “A kinetic-monte carlo perspective on active matter,” *J. Chem. Phys.* **150**, 144113 (2019).
- ⁴¹H. H. Wensink, J. Dunkel, S. Heidenreich, K. Drescher, R. E. Goldstein, H. Löwen, and J. M. Yeomans, “Meso-scale turbulence in living fluids,” *Proc. Natl. Acad. Sci.* **109**, 14308–14313 (2012).
- ⁴²Y. Fily and M. C. Marchetti, “Athermal phase separation of self-propelled particles with no alignment,” *Phys. Rev. Lett.* **108**, 235702 (2012).
- ⁴³I. Buttinoni, J. Bialké, F. Kümmel, H. Löwen, C. Bechinger, and T. Speck, “Dynamical clustering and phase separation in suspensions of self-propelled colloidal particles,” *Phys. Rev. Lett.* **110**, 238301 (2013).
- ⁴⁴J. Palacci, S. Sacanna, A. P. Steinberg, D. J. Pine, and P. M. Chaikin, “Living crystals of light-activated colloidal surfers,” *Science* **339**, 936–940 (2013).
- ⁴⁵J. Bialké, T. Speck, and H. Löwen, “Active colloidal suspensions: Clustering and phase behavior,” *Journal of Non-Crystalline Solids* **407**, 367–375 (2015).
- ⁴⁶M. E. Cates and J. Tailleur, “Motility-induced phase separation,” *Annu. Rev. Condens. Matter Phys.* **6**, 219–244 (2015).
- ⁴⁷G. Gonnella, D. Marenduzzo, A. Suma, and A. Tiribocchi, “Motility-induced phase separation and coarsening in active matter,” *Comptes Rendus Physique* **16**, 316–331 (2015).
- ⁴⁸M. C. Marchetti, Y. Fily, S. Henkes, A. Patch, and D. Yllanes, “Minimal model of active colloids highlights the role of mechanical interactions in controlling the emergent behavior of active matter,” *Curr. Opin. Colloid Interface Sci* **21**, 34–43 (2016).
- ⁴⁹G.-J. Liao and S. H. Klapp, “Clustering and phase separation of circle swimmers dispersed in a monolayer,” *Soft Matter* **14**, 7873–7882 (2018).
- ⁵⁰B. Liebchen and D. Levis, “Collective behavior of chiral active matter: pattern formation and enhanced flocking,” *Phys. Rev. Lett.* **119**, 058002 (2017).

- ⁵¹E. Sese-Sansa, I. Pagonabarraga, and D. Levis, “Velocity alignment promotes motility-induced phase separation,” *EPL* **124**, 30004 (2018).
- ⁵²M. Theers, E. Westphal, K. Qi, R. G. Winkler, and G. Gompper, “Clustering of microswimmers: interplay of shape and hydrodynamics,” *Soft Matter* **14**, 8590–8603 (2018).
- ⁵³J. Stenhammar, A. Tiribocchi, R. J. Allen, D. Marenduzzo, and M. E. Cates, “Continuum theory of phase separation kinetics for active brownian particles,” *Phys. Rev. Lett.* **111**, 145702 (2013).
- ⁵⁴T. Speck, J. Bialké, A. M. Menzel, and H. Löwen, “Effective cahn-hilliard equation for the phase separation of active brownian particles,” *Phys. Rev. Lett.* **112**, 218304 (2014).
- ⁵⁵A. Baskaran and M. C. Marchetti, “Enhanced diffusion and ordering of self-propelled rods,” *Phys. Rev. Lett.* **101**, 268101 (2008).
- ⁵⁶M. Enculescu and H. Stark, “Active colloidal suspensions exhibit polar order under gravity,” *Phys. Rev. Lett.* **107**, 058301 (2011).
- ⁵⁷S. C. Takatori and J. F. Brady, “Inertial effects on the stress generation of active fluids,” *Phys. Rev. Fluids* **2**, 094305 (2017).
- ⁵⁸Z. Mokhtari, T. Aspelmeier, and A. Zippelius, “Collective rotations of active particles interacting with obstacles,” *EPL* **120**, 14001 (2017).
- ⁵⁹S. Shankar and M. C. Marchetti, “Hidden entropy production and work fluctuations in an ideal active gas,” *Phys. Rev. E* **98**, 020604 (2018).
- ⁶⁰A. Manacorda and A. Puglisi, “Lattice model to derive the fluctuating hydrodynamics of active particles with inertia,” *Phys. Rev. Lett.* **119**, 208003 (2017).
- ⁶¹S. Das, G. Gompper, and R. G. Winkler, “Local stress and pressure in an inhomogeneous system of spherical active brownian particles,” *Scientific Reports* **9**, 6608 (2019).
- ⁶²H. D. Vuijk, J.-U. Sommer, H. Merlitz, J. M. Brader, and A. Sharma, “Lorentz forces induce inhomogeneity and fluxes in active systems,” arXiv:1908.02577 (2019).
- ⁶³I. Abdoli, H. D. Vuijk, J.-U. Sommer, J. M. Brader, and A. Sharma, “Nondiffusive fluxes in brownian system with lorentz force,” arXiv:1908.03101 (2019).
- ⁶⁴J. Um, T. Song, and J.-H. Jeon, “Langevin dynamics driven by a telegraphic active noise,” *Frontiers in Physics* **7**, 143 (2019).
- ⁶⁵S. Jahanshahi, A. Ivlev, and H. Löwen, To be published.
- ⁶⁶K. Malakar, A. Das, A. Kundu, K. V. Kumar, and A. Dhar, “Exact steady state of active brownian particles in a 2d harmonic trap,” arXiv:1902.04171 (2019).
- ⁶⁷C. A. Weber, T. Hanke, J. Deseigne, S. Léonard, O. Dauchot, E. Frey, and H. Chaté, “Long-range ordering of vibrated polar disks,” *Phys. Rev. Lett.* **110**, 208001 (2013).
- ⁶⁸H. Löwen, “Active particles in noninertial frames: How to self-propel on a carousel,” *Phys. Rev. E* **99**, 062608 (2019).
- ⁶⁹A. Suma, G. Gonnella, D. Marenduzzo, and E. Orlandini, “Motility-induced phase separation in an active dumbbell fluid,” *EPL* **108**, 56004 (2014).
- ⁷⁰S. Mandal, B. Liebchen, and H. Löwen, “Motility-induced temperature difference in coexisting phases,” *Phys. Rev. Lett.* (in press) (2019).
- ⁷¹I. Petrelli, P. Digregorio, L. F. Cugliandolo, G. Gonnella, and A. Suma, “Active dumbbells: Dynamics and morphology in the coexisting region,” *Eur. Phys. J. E* **41**, 128 (2018).
- ⁷²Y. Komatsu and H. Tanaka, “Roles of energy dissipation in a liquid-solid transition of out-of-equilibrium systems,” *Phys. Rev. X* **5**, 031025 (2015).
- ⁷³D. Helbing, “Traffic and related self-driven many-particle systems,” *Rev. Mod. Phys.* **73**, 1067 (2001).
- ⁷⁴J. Zhang, W. Mehner, E. Andresen, S. Holl, M. Boltes, A. Schadschneider, and A. Seyfried, “Comparative analysis of pedestrian, bicycle and car traffic moving in circuits,” *Procedia - Social and Behavioral Sciences* **104**, 1130–1138 (2013).
- ⁷⁵D. Chowdhury, L. Santen, and A. Schadschneider, “Statistical physics of vehicular traffic and some related systems,” *Phys. Rep.* **329**, 199–329 (2000).
- ⁷⁶J. Bartnick, M. Heinen, A. V. Ivlev, and H. Löwen, “Structural correlations in diffusiophoretic colloidal mixtures with nonreciprocal interactions,” *J. Phys. Condens. Matt.* **28**, 025102 (2016).
- ⁷⁷Y. Levin, “Electrostatic correlations: from plasma to biology,” *Rep. Prog. Phys.* **65**, 1577 (2002).
- ⁷⁸J. Haeberle, J. Harju, M. Sperl, and P. Born, “Granular ionic crystals in a small nutshell,” *Soft matter* **15**, 7179–7186 (2019).
- ⁷⁹N. Casic, N. Quintero, R. Alvarez-Nodarse, F. G. Mertens, L. Jibuti, W. Zimmermann, and T. M. Fischer, “Propulsion efficiency of a dynamic self-assembled helical ribbon,” *Phys. Rev. Lett.* **110**, 168302 (2013).
- ⁸⁰G. Steinbach, S. Gemming, and A. Erbe, “Non-equilibrium dynamics of magnetically anisotropic particles under oscillating fields,” *Eur. Phys. J. E* **39**, 69 (2016).
- ⁸¹A. Nourhani, D. Brown, N. Pletzer, and J. G. Gibbs, “Engineering contactless particle-particle interactions in active microswimmers,” *Adv. Mater.* **29**, 1703910 (2017).
- ⁸²G. Grosjean, M. Hubert, Y. Collard, A. Sukhov, J. Harting, A.-S. Smith, and N. Vandewalle, “Capillary assemblies in a rotating magnetic field,” arXiv:1907.06904 (2019).
- ⁸³R. G. Winkler, J. Elgeti, and G. Gompper, “Active polymersemergent conformational and dynamical properties: A brief review,” *J. Phys. Soc. Jpn.* **86**, 101014 (2017).
- ⁸⁴J. Yan, M. Han, J. Zhang, C. Xu, E. Luijten, and S. Granick, “Reconfiguring active particles by electrostatic imbalance,” *Nature Materials* **15**, 1095 (2016).
- ⁸⁵A. Attanasi, A. Cavagna, L. Del Castello, I. Giardina, T. S. Grigera, A. Jelić, S. Melillo, L. Parisi, O. Pohl, E. Shen, and M. Viale, “Information transfer and behavioural inertia in starling flocks,” *Nature Physics* **10**, 691 (2014).
- ⁸⁶S. Babel, B. ten Hagen, and H. Löwen, “Swimming path statistics of an active brownian particle with time-dependent self-propulsion,” *J. Stat. Mech. Theor. Exp.* **2014**, P02011 (2014).
- ⁸⁷E. Sese-Sansa, I. Pagonabarraga, and D. Levis, “Velocity alignment promotes motility-induced phase separation,” *EPL* **124**, 30004 (2018).
- ⁸⁸R. van Damme, J. Rodenburg, R. van Roij, and M. Dijkstra, “Interparticle torques suppress motility-induced phase separation for rodlike particles,” *J. Chem. Phys.* **150**, 164501 (2019).
- ⁸⁹R. Chatterjee, N. Rana, R. A. Simha, P. Perlekar, and S. Ramaswamy, “Fluid flocks with inertia,” (2019), arXiv:1907.03492.
- ⁹⁰A. Liliushvili, J. Ónody, and T. Voigtman, “Mode-coupling theory for active brownian particles,” *Phys. Rev. E* **96**, 062608 (2017).
- ⁹¹G. Szamel, “Mode-coupling theory for the steady-state dynamics of active brownian particles,” *J. Chem. Phys.* **150**, 124901 (2019).
- ⁹²A. M. Menzel, A. Saha, C. Hoell, and H. Löwen, “Dynamical density functional theory for microswimmers,” *J. Chem. Phys.* **144**, 024115 (2016).
- ⁹³C. Nardini, É. Fodor, E. Tjhung, F. Van Wijland, J. Tailleur, and M. E. Cates, “Entropy production in field theories without time-reversal symmetry: quantifying the non-equilibrium character of active matter,” *Phys. Rev. X* **7**, 021007 (2017).
- ⁹⁴P. Pietzonka and U. Seifert, “Entropy production of active particles and for particles in active baths,” *J. Phys. A* **51**, 01LT01 (2017).
- ⁹⁵S. Krishnamurthy, S. Ghosh, D. Chatterji, R. Ganapathy, and A. Sood, “A micrometre-sized heat engine operating between bacterial reservoirs,” *Nature Physics* **12**, 1134 (2016).
- ⁹⁶D. Martin, C. Nardini, M. E. Cates, and É. Fodor, “Extracting maximum power from active colloidal heat engines,” *EPL* **121**, 60005 (2018).
- ⁹⁷K. Brandner, K. Saito, and U. Seifert, “Thermodynamics of micro- and nano-systems driven by periodic temperature variations,” *Phys. Rev. X* **5**, 031019 (2015).
- ⁹⁸H. Meyer, P. Pelagejcev, and T. Schilling, “Non-markovian out-of-equilibrium dynamics: A general numerical procedure to construct time-dependent memory kernels for coarse-grained ob-

- servables,” arXiv:1905.11753 (2019).
- ⁹⁹J. Berner, B. Müller, J. R. Gomez-Solano, M. Krüger, and C. Bechinger, “Oscillating modes of driven colloids in overdamped systems,” *Nature Commun.* **9**, 999 (2018).
- ¹⁰⁰J. Toner, H. Löwen, and H. H. Wensink, “Following fluctuating signs: Anomalous active superdiffusion of swimmers in anisotropic media,” *Phys. Rev. E* **93**, 062610 (2016).
- ¹⁰¹A. Daddi-Moussa-Ider and A. M. Menzel, “Dynamics of a simple model microswimmer in an anisotropic fluid: Implications for alignment behavior and active transport in a nematic liquid crystal,” *Phys. Rev. Fluids* **3**, 094102 (2018).
- ¹⁰²J. R. Gomez-Solano, A. Blokhuis, and C. Bechinger, “Dynamics of self-propelled janus particles in viscoelastic fluids,” *Phys. Rev. Lett.* **116**, 138301 (2016).
- ¹⁰³R. Piwowarczyk, M. Selin, T. Ihle, and G. Volpe, “Influence of sensorial delay on clustering and swarming,” *Phys. Rev. E* **100**, 012607 (2019).